HTML ABSTRACT + LINKS

In situ real time process characterization in nanoimprint lithography using time-resolved diffractive scatterometry

Zhaoning Yu,[a] He Gao, and Stephen Y. Chou
Nanostructure Laboratory, Department of Electrical Engineering, Princeton University, Princeton, New Jersey 08544

(Received 1 July 2004; accepted 8 September 2004)

To optimize nanoimprint lithography (NIL), it is essential to be able to characterize and control the NIL process *in situ* and in real time. Here, we present a method for *in situ* real-time NIL process characterization using time-resolved diffractive scatterometry (TRDS). A surface relief diffraction grating is used as the imprint mold, and the diffracted light intensity is monitored continuously during the imprint process. We use a scalar diffraction model to calculate the diffraction intensity as a function of the mold penetration ratio. Simulations show good agreement with the experimental results. Our results indicate that TRDS offers a powerful characterization tool that can be used for *in situ*, real-time NIL process control. © *2004 American Institute of Physics*.
[DOI: 10.1063/1.1811396]

Nanoimprint lithography (NIL) is a promising technology that has the potential to become a low-cost high throughput lithography tool for the mass production of nanoscale devices and systems.[1] It has demonstrated sub-10 nm resolution and has been applied to the fabrication of a variety of nanodevices in different fields.[1–4]

NIL patterns by physically deforming a polymer resist thin film using a mold. The resist can be either thermoplastic or photocurable.[1,5] A thermoplastic resist is initially in a solid form at a low temperature and becomes viscous when heated above its glass transition temperature (T_g) during imprinting. For a photocurable resist, it is initially in a liquid form and becomes solid after curing. Clearly, polymer deformation plays a critical role in nanoimprint lithography. To optimize NIL, it is essential to characterize and control the deformation of the resist *in situ* and in real time. However, currently, few studies on this subject have been carried out or reported.

Here, we present a method for *in situ* real-time NIL process characterization using time-resolved diffractive scatterometry (TRDS). We report on its application in characterizing the nanoimprint process. In TRDS, a surface relief diffraction grating is used as the imprint mold, and the diffracted light intensity is monitored continuously during the imprint process. We use a scalar diffraction model to calculate the diffraction intensity as a function of the mold penetration ratio, simulations show good agreement with the experimental results. Our results indicate that TRDS offers a powerful characterization tool that can be used for *in situ* real-time NIL process control.

Figure 1 shows a schematic of the TRDS setup we use to detect the NIL process. Previously, optical scatterometry was used in surface analysis, and diffraction-based interferometry was used in measuring the mask-wafer gap.[6–8] In the TRDS experiment, a surface-relief diffraction grating was patterned on an imprint mold made of a transparent fused silica substrate with a thickness of 0.5 mm. The grating mold is fabricated using a process combining interference lithography, NIL, wet etch, and reactive ion etching to achieve the desired sidewall smoothness and grating linewidth.[9] Figure 2 is a scanning electron micrograph (SEM) showing a cross-sectional view of the fused silica grating mold used in the experiment to be discussed in this letter: The 1.0 μm period grating has a rectangular profile, with a linewidth of 650 nm and a pattern depth of 400 nm.

During the TRDS measurement, the transparent grating mold is placed on top of the polymer thin film spincoated on a silicon substrate, a He–Ne laser beam with a wavelength of 632.8 nm is incident upon the grating area (at an incident angle of 30°, with the grating lines parallel to the plane of incidence), and the intensity of the diffracted light is monitored continuously during the NIL process (Fig. 1). The imprint is performed using a modified NX-2000 imprint system (Nanonex Corp., Monmouth Junction, New Jersey), which provides precise control of the applied pressure and the temperature of the sample during an imprint process.

The experimentally measured first-order diffraction intensity and sample temperature in a typical TRDS measurement are shown in Fig. 3. At the start of the imprint process, the mold and the substrate are brought into contact by external pressure (throughout this NIL experiment, a constant pressure of 5.1×10^5 Pa is applied) at room temperature. The polymer is rigid at this temperature and the pressure alone cannot deform the resist, so the measured diffraction intensity stabilizes at an initial value. Next, the resist and mold are heated up, the polymer softens, the mold is gradually imprinted into the resist under the applied pressure, and the first-order diffraction intensity decreases. Upon completion

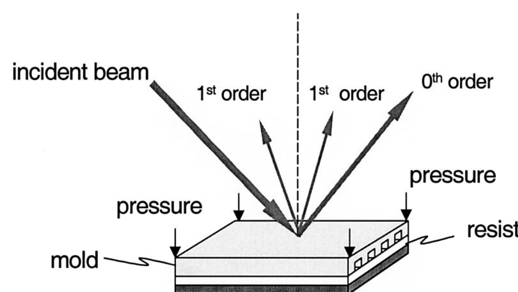

FIG. 1. Schematic of NIL characterization using TRDS: Intensity of the first-order diffraction is monitored continuously during the NIL process.

[a]Electronic mail: zhyu@princeton.edu

 © 2004 American Institute of Physics
Downloaded 17 Mar 2006 to 128.112.49.128. Redistribution subject to AIP license or copyright, see http://apl.aip.org/apl/copyright.jsp

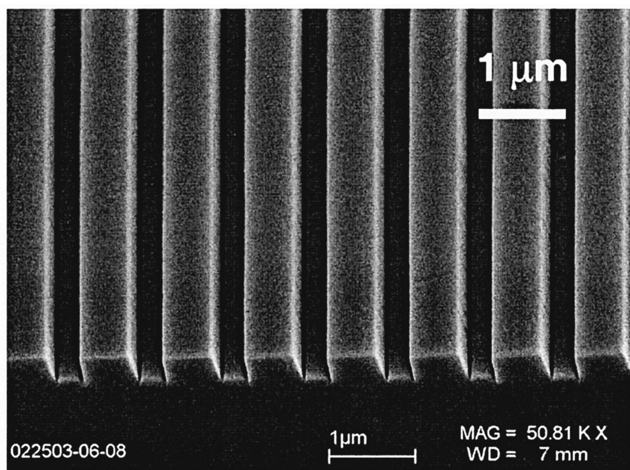

FIG. 2. SEM showing a cross-sectional view of the fused silica 1.0 μm period diffraction grating mold used in the TRDS experiment.

of the imprint, the grooves are completely filled by the polymer, and the diffraction intensity reaches its near-zero minimum because of the close match between the refractive indices of the polymer (1.46) and the fused silica mold (1.46). Data in Fig. 3 show that the TRDS clearly distinguish the start and endpoint of the imprint, allowing us *in situ* real-time monitoring of the NIL process, from which important information such as the speed of mold penetration can be extracted.

To obtain a clear picture of the NIL process from TRDS measurements, it is necessary to relate the measured optical intensity with the degree of mold penetration into the resist in NIL. Although rigorous numerical simulations are highly desirable, we have found that a much simpler scalar diffraction theory[10,11] is generally sufficient for a good approximation in our case.

Figure 4 shows a schematic of the NIL system to be analyzed in this study. The grating has a period of p_m, a trench width of w_m, and a trench depth of h_m. The initial resist thickness is h_r. During NIL, the mold is pressed into the polymer under external pressure P, the mold penetration depth h_p is defined as the height of the resist protruding into the mold grooves. The penetration ratio R_p is defined as the ratio of penetration depth h_p to the mold depth $h_m (R_p = h_p/h_m)$. The penetration ratio R_p changes from 0 to 1 during a NIL process. At the start of NIL, the resist is not deformed and there is no polymer protruding into the mold grooves, so $R_p=0$; at the end of the NIL, the mold grooves are completely filled by the resist, so $R_p=1$.

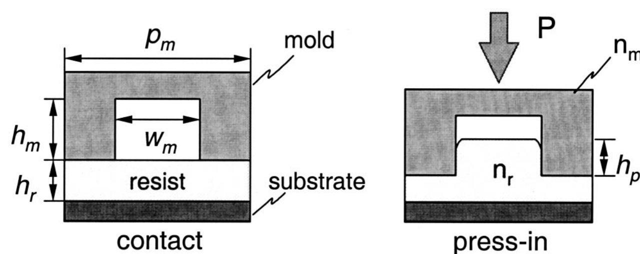

FIG. 4. Schematic of the NIL system to be analyzed.

Figure 5 shows the simulated first-order diffraction intensity as a function of the mold penetration ratio R_p calculated using the scalar diffraction theory. Cross-sectional SEM of the grating (Fig. 2) is used to determine the mold parameters used in our simulation: Grating period $p_m=1.0$ μm, trench width $w_m=350$ nm, and trench depth $h_m=400$ nm. We have also assumed a wavelength λ of 632.8 nm, and that the resist has a sufficient initial thickness $h_r > 200$ nm so that there is enough resist to completely fill the trench groove volume at the end of the NIL.

Our simulation shows that the characteristics of the (diffraction intensity)–(mold penetration ratio) dependence are affected by the mismatch between the refractive indices of the mold material (fused silica in our case with a refractive index $n_m=1.46$) and the resist (n_r). Specifically, when n_r is a perfect match to n_m ($n_r=n_m=1.46$, shown as the solid line in Fig. 5), diffraction intensity decreases continuously with increasing R_p and reaches 0 at the end of NIL. However, when there is a mismatch between n_r and n_m, the final value of diffraction intensity corresponding to the end of NIL ($R_p=1.0$) is always higher than zero. For example, we have calculated the case when $n_r=1.58$ (the dashed line in Fig. 5), which is significantly higher than the index of the mold material (fused silica, $n_m=1.46$). In such a case, the diffraction intensity reaches zero when the mold grooves are partially filled ($R_p \sim 0.8$) and it increases slightly toward the end of

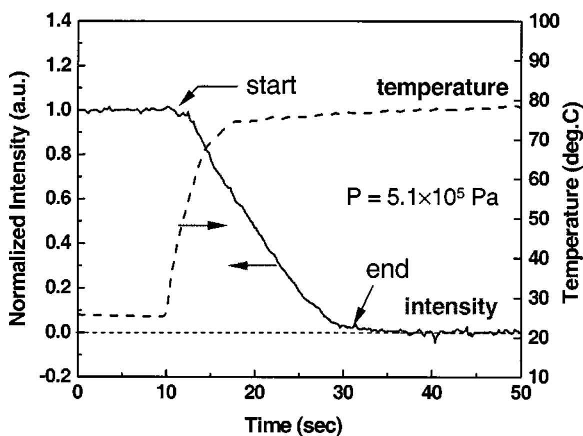

FIG. 3. Experimentally measured first-order diffraction intensity and sample temperature as functions of time during a NIL process. The TRDS measurement clearly shows the start and endpoint of the imprint process, from which information on the speed of mold penetration can be extracted.

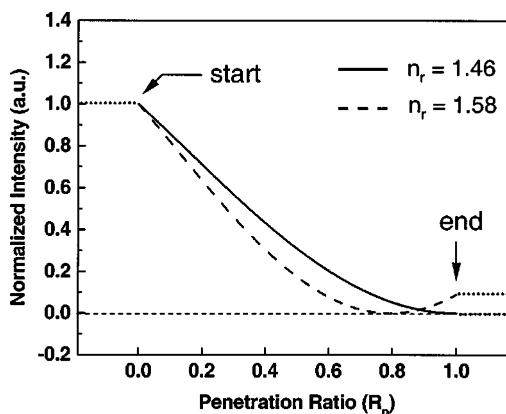

FIG. 5. Simulated first-order diffraction intensity as a function of mold penetration ratio calculated using the scalar diffraction model: When refractive indices of the mold (n_m) and resist (n_r) match each other ($n_m=n_r=1.46$), diffraction intensity decreases to zero at the end of NIL ($R_p=1.0$). However, when n_r is significantly higher than n_m ($n_r=1.58$ and $n_m=1.46$), a minimum in diffraction intensity does not correspond to the NIL endpoint.

Downloaded 17 Mar 2006 to 128.112.49.128. Redistribution subject to AIP license or copyright, see http://apl.aip.org/apl/copyright.jsp

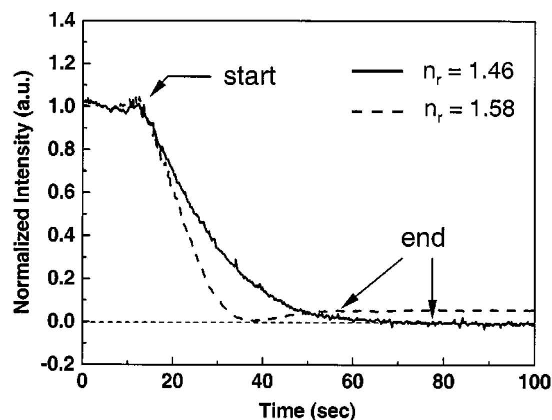

FIG. 6. Experimentally measured first-order diffraction intensities during NIL as functions of time for resists with different indices of refraction (1.46 and 1.58). The experiment confirms the predictions given by the scalar diffraction model (Fig. 5).

the NIL when R_p increases to its final value of 1.0.

We have found the scalar diffraction model to be a good approximation in quantitatively evaluating the diffraction intensity as a function of mold penetration. It also helps to qualitatively explain characteristics of the data obtained in the TRDS measurement. Figure 6 shows the experimentally measured first-order diffraction intensity as a function of time during a NIL process for resists with different refractive indices. The same grating mold shown in Fig. 2 was used in these experiments. Two types of commercially available thermoplastic polymer resist (provided by Nanonex Corp.) were used: Resist No. 1 has a refractive index $n_r = 1.46$; Resist No. 2 has a refractive index $n_r = 1.58$ (determined by ellipsometry). In both of these experiments, the polymer thin film has the same initial thickness (h_r) of $\sim$210 nm. Because of the difference in their glass transition temperatures, the two resists were imprinted under different conditions so that the NIL process would have a comparable duration in time for both cases. Resist No. 1 was imprinted at a pressure of 7.9×10^5 Pa and a temperature of 60 °C. Resist No. 2 was imprinted at a pressure of 6.5×10^5 Pa and a temperature of 80 °C. The data clearly show that when n_r matches n_m, the diffraction intensity drops to zero at the end of NIL (resist No. 1, solid line in Fig. 6). However, when n_r is higher than n_m, the diffraction intensity reaches zero before the mold grooves are completely filled and approaches its nonzero final value at the end of NIL (Resist No. 2, dashed line in Fig. 6). The experiment confirms the predictions given by the scalar diffraction model shown in Fig. 5.

In summary, we have presented an approach to *in situ* real-time NIL process characterization using TRDS. A surface relief diffraction grating is used as the imprint mold, and the diffracted light intensity is monitored continuously during the imprint process. We have also used a scalar diffraction model to calculate the diffraction intensity as a function of the mold penetration ratio. Simulations show good agreement with the experimental results. Our results indicate that TRDS offers a useful tool for *in situ* real-time NIL process detection and control.

This work was partially supported by DARPA and ONR.

[1]S. Y. Chou, P. R. Krauss, and P. J. Renstrom, Science **272**, 85 (1996).
[2]M. Li, L. Chen, and S. Y. Chou, Appl. Phys. Lett. **78**, 3322 (2001).
[3]D. S. Macintyre, Y. Chen, D. Lim, and S. Thoms, J. Vac. Sci. Technol. B **19**, 2797 (2001).
[4]L. J. Guo, X. Cheng, and C. Chou, Nano Lett. **4**, 69 (2004).
[5]Y. Hirai, M. Fujiwara, T. Okuno, Y. Tanaka, M. Endo, S. Irie, K. Nakagawa, and M. Sasago, J. Vac. Sci. Technol. B **19**, 2811 (2001).
[6]C. Raymond, M. Murnane, S. Prins, S. Sohail, H. Naqvi, J. McNeil, and J. Hosch, J. Vac. Sci. Technol. B **15**, 361 (1997).
[7]S. Sohail, H. Naqvi, S. Zaidi, S. Brueck, and J. McNeil, J. Vac. Sci. Technol. B **12**, 3600 (1994).
[8]E. Moon, P. Everett, M. Meinhold, M. Mondol, and H. Smith, J. Vac. Sci. Technol. B **17**, 2698 (1999).
[9]Z. Yu and S. Y. Chou, Nano Lett. **4**, 341 (2004).
[10]R. L. Morrison, J. Opt. Soc. Am. A **9**, 464 (1992).
[11]M. Born and E. Wolf, *Principles of Optics*, 7th ed. (Cambridge University Press, Cambridge, U.K., 1999), p. 413.

Downloaded 17 Mar 2006 to 128.112.49.128. Redistribution subject to AIP license or copyright, see http://apl.aip.org/apl/copyright.jsp